

# “Anion-Switchable” Pincer-Mn(I) Catalyst for the Reductive N-Methylation of Amines with Formic Acid and CO<sub>2</sub>

Sebastián Martínez-Vivas, Sergio Gonell, Macarena Poyatos,\* and Eduardo Peris\*



Cite This: *ACS Catal.* 2024, 14, 7600–7608



Read Online

ACCESS |



Metrics & More



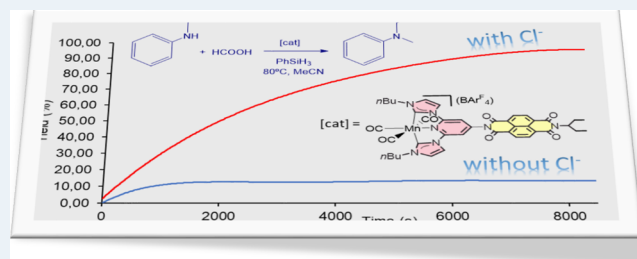
Article Recommendations



Supporting Information

**ABSTRACT:** We report a manganese(I) complex of formula [Mn(NDI-CNC)(CO)<sub>3</sub>](BAR<sup>F</sup><sub>4</sub>), in which NDI-CNC refers to a pincer pyridine-bis-imidazolylidene ligand functionalized with a naphthalene-diimide (NDI) moiety. Due to the presence of the NDI fragment, the electron-donating strength of the pincer ligand can be increased by producing an electrochemical reduction of the NDI moiety or by the addition of tetrabutylammonium chloride (TBACl). The extent of the changes produced in the electron-donating power of the pincer ligand can be quantified by studying the variation of the C–O stretching frequencies by infrared spectroscopy. It is observed that the catalytic activity of the manganese complex in the reductive methylation of a series of secondary amines with formic acid (or CO<sub>2</sub>) in the presence of PhSiH<sub>3</sub> is almost negligible, but the catalyst can be turned very active in the presence of TBACl. This study constitutes a rare example of an anion-sensitive catalyst. Furthermore, the activity of the catalyst can be switched on and off for several cycles by subsequent addition of TBACl or NOBF<sub>4</sub>, respectively.

**KEYWORDS:** manganese, CO<sub>2</sub> reduction, methylation of amines, pincer ligands, switchable catalysts, anion-sensitive ligands



It is observed that the catalytic activity of the manganese complex in the reductive methylation of a series of secondary amines with formic acid (or CO<sub>2</sub>) in the presence of PhSiH<sub>3</sub> is almost negligible, but the catalyst can be turned very active in the presence of TBACl. This study constitutes a rare example of an anion-sensitive catalyst. Furthermore, the activity of the catalyst can be switched on and off for several cycles by subsequent addition of TBACl or NOBF<sub>4</sub>, respectively.

## INTRODUCTION

Due to its abundance in the earth's crust and to the wide range of possible available oxidation states, during the past few years, manganese has proven to be an attractive candidate for new catalyst development,<sup>1</sup> although some authors have recently pointed out drawbacks because the lack of efficient recycling methods may cause a risk in the supply chain.<sup>2</sup> Among manganese-based homogeneous catalysts, those supported by pincer ligands have recently proven successful in a very large number of organic transformations.<sup>1c,g,3</sup> Well-defined manganese(I) complexes supported by N-heterocyclic carbene (NHC) ligands have been explored in the electrocatalytic CO<sub>2</sub> reduction as well as in reactions that fall into the so-called diagonal transformation of CO<sub>2</sub>,<sup>4</sup> which involves its simultaneous reduction and functionalization. Agarwal et al. were the first to describe two NHC-based manganese(I) compounds that were used for the electroreduction of CO<sub>2</sub> to CO.<sup>5</sup> The electronic properties of these catalysts, which contained a pyridine-NHC ligand, were further tuned by changing the axial bromide ligand<sup>6</sup> and the nature of the NHC.<sup>7</sup> Soon thereafter, Royo and Lloret disclosed the extraordinary activity and selectivity of a Mn-based catalyst bearing a bidentate methylene-bridged bis-imidazolylidene ligand toward the electroreduction of CO<sub>2</sub> to CO,<sup>8</sup> and unveiled the factors that govern its reactivity and selectivity.<sup>9</sup> This Mn(I)-bisNHC complex was also found to be active in the reductive N-formylation and N-methylation of secondary amines using either CO<sub>2</sub> or formic acid as C<sub>1</sub> building blocks, showing

remarkable selectivity to the N-methylated products.<sup>10</sup> Luca and co-workers showed that pincer Mn(I) complexes were particularly effective in the electrocatalytic reduction of CO<sub>2</sub>,<sup>11</sup> and performed detailed mechanistic studies.<sup>11b,12</sup> In a more recent study, it was found that the introduction of electron-donating groups at the *para* position of the pyridine ring revealed a much more active catalyst for the electrocatalytic reduction of CO<sub>2</sub>, thus highlighting that the tuning of the electronic properties of the ligand has a large impact on the performance of the catalyst.<sup>13</sup>

These approaches for chemical or electrochemical CO<sub>2</sub> valorization using earth-abundant Mn complexes are heralding the nascence of the area of catalysis with Mn-NHC complexes.<sup>14</sup> Indeed, a plethora of catalytic applications of manganese complexes has been reported over the past few years, including hydrosilylation<sup>15</sup> and hydrogenation reactions,<sup>16</sup> to name just a couple.

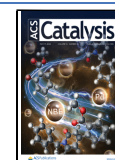
Naphthalene-diimides (NDIs) are known to show unique redox and electrochemical properties.<sup>17</sup> In addition, the electron-deficient nature of NDIs makes them particularly suited for engaging in anion- $\pi$  interactions,<sup>18</sup> a property that

Received: March 25, 2024

Revised: April 15, 2024

Accepted: April 17, 2024

Published: May 1, 2024



## Scheme 1. Synthesis of Mn(I) Pincer Complexes 2 and 4

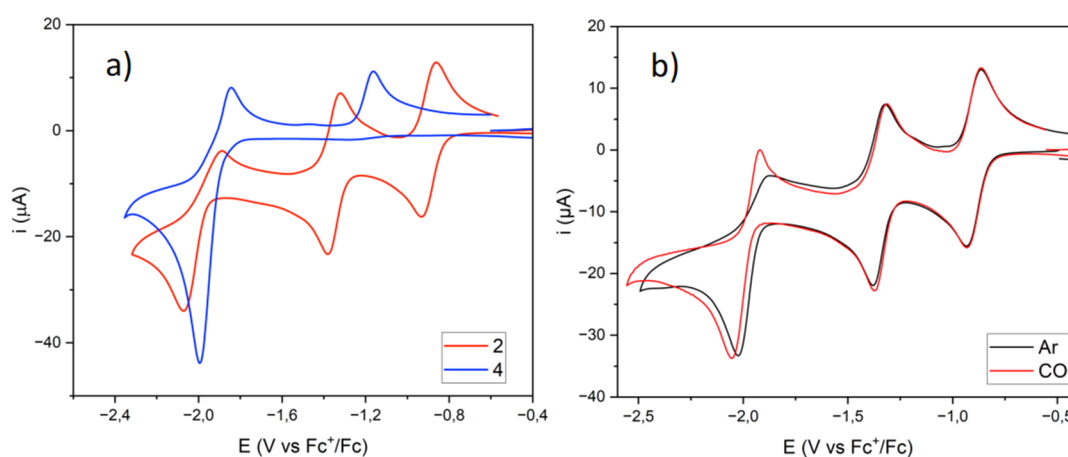
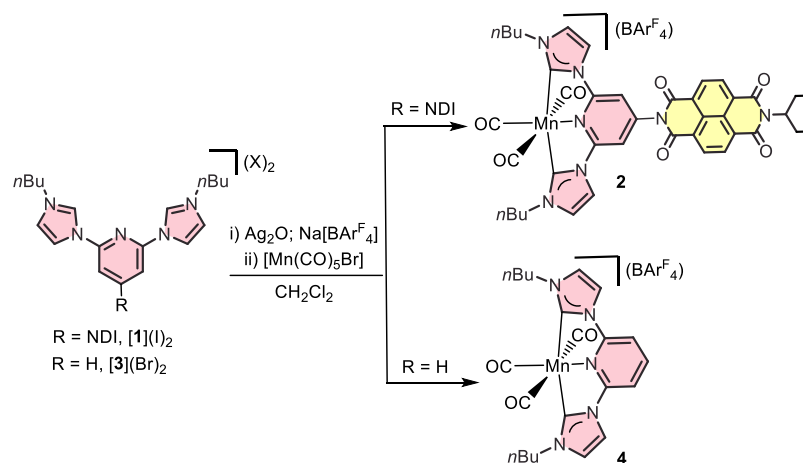


**Figure 1.** (a) Cyclic voltammetry of **2** (red) and **4** (blue) in dry acetonitrile and 0.1 M  $[\text{N}(\text{nBu})_4][\text{PF}_6]$  under an Ar atmosphere. (b) Cyclic voltammetry of **2** in dry acetonitrile and 0.1 M  $[\text{N}(\text{nBu})_4][\text{PF}_6]$  under Ar (black) and CO (red) atmospheres. Measurements were performed at 100 mV/s and referenced against ferrocene/ferrocenium.

turned out to be very useful in their application in the domain of anion sensing.<sup>19</sup>

In our preliminary attempts to merge the properties of NDIs with those of NHCs in homogeneous catalysis, we first designed directly fused NDI-NHC ligands and demonstrated that their related complexes could be successfully employed as redox-switchable catalysts in the cycloisomerization of alkynoic acids<sup>20</sup> and in the hydroamination of acetylenes.<sup>21</sup> Our studies revealed that the NDI moiety behaved as a redox-switchable tag that allowed modification of the electron-donating strength of the ligands in a controlled and reversible manner. More recently, we showed how a rhodium(I) complex with an NDI-functionalized NHC-based pincer ligand could improve its catalytic activity by adding fluoride, which turned out to behave as a very effective redox stimulus.<sup>22</sup>

Building on these grounds, we herein report the preparation of a Mn(I) complex supported by an NDI-functionalized NHC-based pincer CNC ligand and the study of its catalytic performance in the reductive *N*-methylation of a series of secondary amines using formic acid or  $\text{CO}_2$ . The effect of modulating the electronic properties of the NDI-functionalized pincer Mn(I) complex by the addition of fluoride will be described and discussed.

## RESULTS AND DISCUSSION

The NDI-pincer Mn(I) complex **2** was prepared by reacting the NDI-functionalized bis-imidazolium salt  $[\mathbf{1}](\text{I})_2$ <sup>22</sup> with  $\text{Ag}_2\text{O}$  in  $\text{CH}_2\text{Cl}_2$ , and then by transmetalating the in situ generated silver-NHC complex with  $[\text{Mn}(\text{CO})_5\text{Br}]$  in the presence of  $\text{Na}(\text{BAr}^{\text{F}}_4)$ , as shown in Scheme 1. For comparative purposes and following the same synthetic route, we also prepared complex **4**, lacking the NDI functionalization, starting from  $[\mathbf{3}](\text{Br})_2$ . Complexes **2** and **4** were characterized by NMR and IR spectroscopy and mass spectrometry, and gave satisfactory elemental analysis. The  $^{13}\text{C}$  NMR spectrum of **2** shows two signals assigned to the carbonyl ligands at 208.2 and 206.2 ppm. The resonance due to the carbene carbon is observed at 204.1 ppm. The IR spectrum of **2** shows the characteristic bands corresponding to a *mer* arrangement of the three carbonyl ligands at 2051, 1968, and 1914  $\text{cm}^{-1}$ , at slightly higher frequencies than those shown by complex **4** (2049, 1965, and 1912  $\text{cm}^{-1}$ ), as should be expected due to the presence of the electron-deficient NDI moiety in the pincer ligand of **2**.

Electrochemistry of complexes **2** and **4** was carried out in a 0.1 M acetonitrile solution of tetrabutylammonium hexafluorophosphate ( $\text{TBAPF}_6$ ), using a glassy carbon working electrode, a platinum wire counter-electrode, and a silver wire pseudoreference electrode. Unless otherwise stated, all of

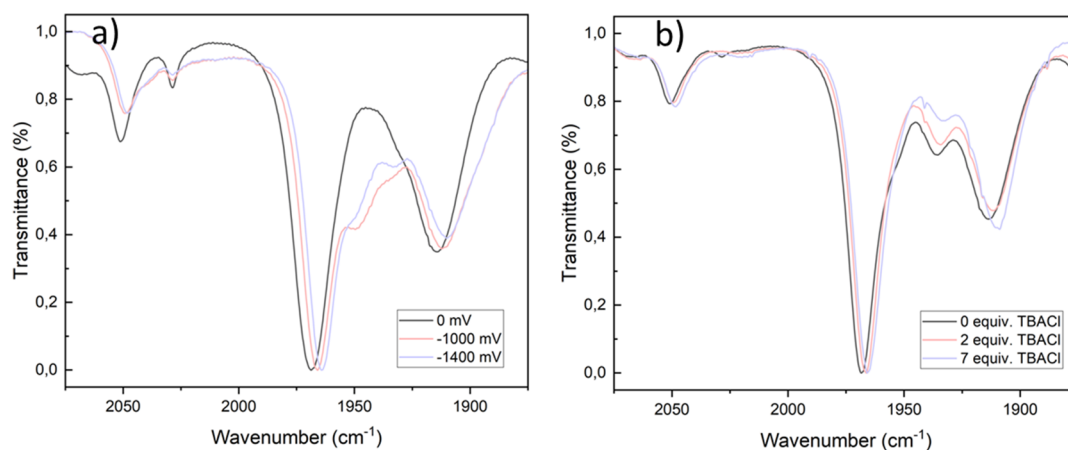


**Figure 2.** (a) IR-SEC reduction of **2** in dry  $\text{CH}_3\text{CN}$  (0.1 M  $[\text{N}(\text{nBu})_4][\text{PF}_6]$ ). The solid lines represent the IR spectra of complex **2** (black), one-electron reduced species (red), and two-electron reduced species (blue). (b) IR spectroscopic changes in the spectrum of **2** observed upon the addition of different amounts of chloride [0 equiv of TBACl (black), 2 equiv of TBACl (red), and 7 equiv of TBACl (blue)].

the measurements were conducted under argon at 100 mV/s, and the potentials were referenced against the ferrocene/ferrocenium couple (Figure 1a). As observed for other related pincer-CNC tricarbonyl complexes of Mn(I),<sup>11,13</sup> the cyclic voltammogram of **4** shows a metal-centered one-electron irreversible reduction event at  $-1.99$  V. As established for related cationic (CNC)-Mn(I) carbonyl compounds, this species may have a radical character on the metal, but with significant delocalization on the ligand.<sup>11b</sup> It has been hypothesized that this neutral radical may undergo incomplete dimerization,<sup>11a,23</sup> after the loss of two carbonyl ligands.<sup>11b</sup> The slight feature observed on the return scan at  $-1.2$  V corresponds to oxidation of the dimetallic species formed.

Complex **2** shows two well-separated reversible reduction waves at  $-0.89$  and  $-1.35$  V, which correspond to the sequential one- and two-electron reductions of the NDI core. A third irreversible reduction wave observed at  $-2.07$  V is associated with the reduction of the manganese center, with the concomitant loss of two carbonyl ligands. The cathodic shift of about 70 mV of this reduction peak with respect to that shown by complex **4** indicates that the 2-electron reduction of the NDI core has a small but non-negligible influence on the reduction of the metal center. A cyclic voltammogram of **4** under a CO atmosphere makes the feature attributed to the reduction of the Mn center become quasi-reversible, strongly indicating that the irreversibility of this event is due to CO loss (see Figure 1b).

In order to evaluate the influence of the reduction of the NDI moiety on the electron-donating character of the NDI-pincer ligand in **2**, we decided to perform infrared spectroelectrochemical (IR-SEC) studies. The experiment was performed in acetonitrile by applying progressively more negative potentials to a solution of **2** while recording the corresponding IR spectra. As can be observed from the series of spectra shown in Figure 2a, upon one-electron reduction of the NDI moiety, all three CO stretching bands reduce their frequencies by  $3\text{ cm}^{-1}$ . Further reduction at more negative potentials produced a further  $3\text{ cm}^{-1}$  decrease in the C–O frequencies. This experiment indicates that the reduction of the NDI moiety at the CNC ligand can be used for increasing the electron-donating power of the pincer ligand. We also performed the same experiment using complex **4** and observed that the application of potentials between  $0$ –( $-1.5$  V) did not

produce any detectable effect on the CO stretching frequencies of this complex (Figure S13 in ESI).

Given the ability of NDI-containing compounds to engage anion- $\pi$  interactions,<sup>19</sup> we decided to study the effect of adding tetrabutylammonium chloride (TBACl) on the IR spectrum of **2**. As can be observed in the series of spectra shown in Figure 2b, the addition of increasing amounts of TBACl (0–7 equiv) to a  $\text{CH}_3\text{CN}$  solution of **2** has the same exact effect as the electrochemical one-electron reduction (2 equiv of TBACl) and two-electron reduction (7 equiv of TBACl) of the complex, as the same shifts on the C–O stretching bands were observed. This experiment indicates that the addition of chloride anion to a solution of **2** has an effect on the electron-donating character of the NDI-pincer ligand similar to that of the electrochemical reduction of the NDI core. On the other hand, we observed that the addition of TBACl did not produce any changes on the CO stretching frequencies of complex **4** (Figure S16 in ESI), thus indicating that the interaction of the chloride anion was produced only on the NDI moiety of complex **2**, and not on the metal.

We also monitored the addition of TBACl to a  $\text{CD}_3\text{CN}$  solution of **2** by  $^1\text{H}$  NMR spectroscopy and observed that the addition of increasing amounts of chloride resulted in the gradual disappearance of the signals due to the protons of the NDI core of the pincer ligand (see Figure S18 in the ESI), strongly suggesting the formation of a paramagnetic species with one electron located at the NDI moiety. This experiment indicates that the interaction of the chloride anion with the complex is capable of producing one-electron reduction of the NDI core, forming an anionic  $\text{NDI}^{\cdot-}$  radical. In order to give further support to this conclusion, we also performed a UV–vis spectroelectrochemical study of complex **2**. The experiment was performed in acetonitrile by applying negative potentials to a solution of **2** while recording the corresponding UV–vis spectra (see Figure S14 in ESI). In a parallel experiment, we studied the UV–vis changes produced in a  $\text{CH}_3\text{CN}$  solution of **2** upon the addition of increasing amounts of TBACl (see Figure S17 in ESI). The comparison of the UV–vis spectra of the species formed upon producing the one-electron reduction of **2** and the one formed upon the addition of 5 equiv of TBACl clearly indicates that the product formed by these two methods is the same, thus indicating that the addition of TBACl produces the one-electron reduction of **2**.

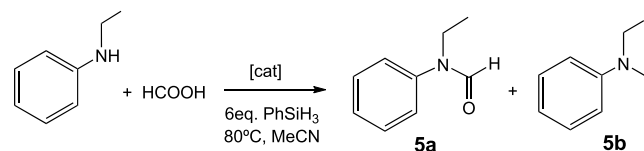
This observation is in agreement with the studies performed by Saha and co-workers, who demonstrated that the addition of  $\text{Cl}^-$  can generate the  $\text{NDI}^-$  radical anion,<sup>24</sup> although the mechanism for this type of electron-transfer process is still a matter of strong debate.

When we monitored the addition of increasing amounts of TBACl to a  $\text{CD}_3\text{CN}$  solution of **4**, we did not observe changes in the  $^1\text{H}$  NMR spectrum of the complex, thus confirming that all changes observed when **2** was used should be assigned to the interaction of the anion with its NDI moiety.

We next wanted to study whether the enhancement of the electron-donating properties of the NDI-pincer ligand in **2** upon the addition of chloride could be translated into a modification of the catalytic properties of the complex. We first decided to study the *N*-methylation of secondary amines using formic acid as the  $\text{C}_1$  building block and a silane as a reducing agent. This reaction, first reported by Beller and co-workers in 2014 using Karstedt's catalyst,<sup>25</sup> allows the preparation of tertiary amines under relatively mild conditions. This reaction is mechanistically related to the reductive formylation and methylation of amines with  $\text{CO}_2$ ,<sup>26</sup> which was reported for the first time in 2012 by Cantat and co-workers who showed that the process can proceed by both, an organometallic or organo-catalytic pathway.<sup>27</sup> During the past few years, several manganese-based catalysts have proven to be highly effective for this type of transformation.<sup>10,28</sup> The *N*-methylation reaction involves two steps. First, formylation of the secondary amine is produced to form a formamide, which is further reduced to form a methyl amine in the second step. The second step is more challenging than the first one,<sup>29</sup> thus providing a good opportunity for studying the selectivity of the process.

We first studied the reaction between *N*-ethylaniline and formic acid in the presence of six equivalents of  $\text{PhSiH}_3$  as the reducing agent. We chose this model substrate because we found that the reaction outcome could be very easily monitored by  $^1\text{H}$  NMR spectroscopy, as all of the products and starting reagents were easily identified in the spectra. The reactions were carried out in  $\text{CH}_3\text{CN}$  at  $80^\circ\text{C}$ , and the analysis of the reaction products was performed by  $^1\text{H}$  NMR spectroscopy after three h of reaction. As can be observed from the results shown in Table 1, both catalysts **2** and **4** show almost identical activities, as they both provided moderate conversions, with a very poor selectivity toward the methylated amine **5b** (see entries 1 and 2). The addition of tetrabutylammonium chloride (TBACl, 20 mol %) as a chloride source produced a clear enhancement of the catalytic performance of the NDI-functionalized catalyst **2**. As can be observed from the data shown in Table 1, when 5 mol % of **2** was used, the addition of TBACl provided full conversion and almost quantitative production of the methylated amine **5b**, and only traces (<5%) of the formylated amine **5a** were detected (entry 4). The reduction of the catalyst load to 2.5 and 1 mol %, provided a decrease in the conversion and selectivity toward **5b**, although the methylated amine was still obtained as the major product. Interestingly, when TBACl was added to the reaction catalyzed by **4**, the conversion increased significantly compared to the reaction performed using the same catalyst in the absence of TBACl, but the reaction was still selectively producing the formylated amine **5a**, with a very poor production of **5b** (compare entries 2 and 7). For the reaction performed using TBACl alone, a high conversion of 88% was achieved, but only traces of methylated product **5b**

**Table 1.** Formylation/Methylation of *N*-Ethylaniline<sup>a</sup>



| entry | cat/load             | additive | conv/% | 5a (%) | 5b (%) |
|-------|----------------------|----------|--------|--------|--------|
| 1     | <b>2</b> (5 mol %)   | none     | 58     | 45     | 13     |
| 2     | <b>4</b> (5 mol %)   | none     | 59     | 49     | 10     |
| 3     | none                 | TBACl    | 88     | 84     | 4      |
| 4     | <b>2</b> (5 mol %)   | TBACl    | 100    | 6      | 94     |
| 5     | <b>2</b> (2.5 mol %) | TBACl    | 92     | 17     | 75     |
| 6     | <b>2</b> (1 mol %)   | TBACl    | 79     | 37     | 42     |
| 7     | <b>4</b> (5 mol %)   | TBACl    | 88     | 80     | 8      |

<sup>a</sup>Reaction conditions: In a thick-walled glass tube fitted with a Teflon cap, the catalyst was added to a 0.081 M solution of *N*-ethylaniline (0.081 mmol), phenylsilane (0.486 mmol), formic acid (0.243 mmol) in  $\text{CH}_3\text{CN}$  (1 mL). For entries 3–7, the amount of TBACl used was 20 mol %. The reaction mixture was allowed to react at  $80^\circ\text{C}$  for 3 h. The products were analyzed by  $^1\text{H}$  NMR spectroscopy taking aliquots (20  $\mu\text{L}$ ) at the desired times using 1,3,5-trimethoxybenzene as integration standard. The results shown are the average between two runs.

were obtained (entry 3). It needs to be mentioned that halides are known to be able to catalyze the reductive formylation of amines with formic acid and silanes, although only fluoride is able to produce the targeted methylated product.<sup>30</sup> In our case, the observation that TBACl alone shows almost identical activity to the combination of **4** and TBACl, indicates that there is no synergistic benefit in mixing these two cocatalysts together. On the contrary, the quantitative production of **5b** upon mixing **2** and TBACl is a clear indication that the NDI moiety present in **2** plays a crucial role in the improvement of the catalytic outcome of this manganese catalyst and that the metal catalyst is key in the reduction of the formylated amine to the methylated amine. It needs to be mentioned that the addition of larger amounts of chloride (>4 equiv with respect to **2**), did not produce any further enhancement of the activity of **2**.

In order to check if the catalytic enhancement produced by the addition of TBACl could also be influenced by the employed amine, we performed a screening of the reaction using different secondary amines using **2** as catalyst. As can be observed from the results shown in Table 2, in all cases, catalyst **2** alone produced mainly the formylated product, while the combination of **2** and TBACl greatly improved the selective formation of the final methylated product.

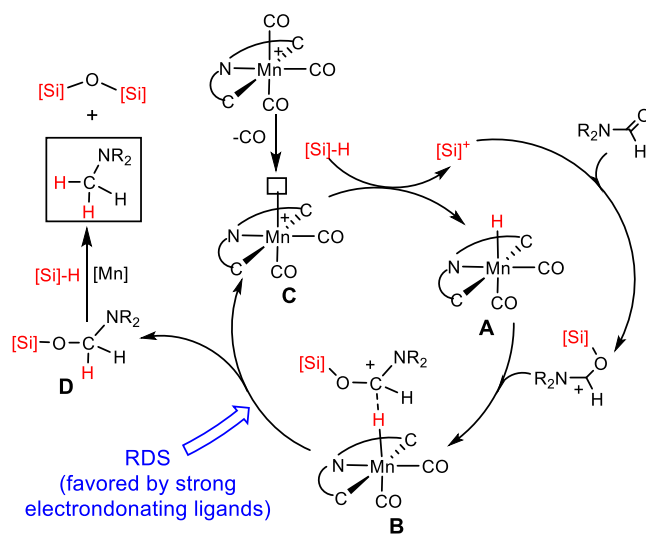
Aiming to provide a better insight into the beneficial effect of the addition of TBACl to the catalytic activity of **2**, we decided to perform some further experiments. First, we decided to determine the reaction rate order with respect to the catalyst using the variable time normalization analysis, which consists of the visual comparison of the variably normalized concentration profiles.<sup>31</sup> The reactions were performed using three catalyst loadings (1, 2.5, and 5 mol %) while maintaining a constant concentration of the TBACl additive (20 mol %), so that the combined analysis of the profiles provided us with information about the changes in the concentration of the metal catalyst alone. The normalized profiles matched with first order in **2** (see Figure S22 in ESI), thus indicating that the production of the methylated amine **5b**

**Table 2. Formylation/Methylation of Different Amines Using 2**

| Entry | Amine | Additive | Conversion (%) | Formylated product (%) | Methylated product (%) |
|-------|-------|----------|----------------|------------------------|------------------------|
| 1     |       | none     | 58             | 45                     | 13                     |
| 2     |       | TBACl    | 100            | 6                      | 94                     |
| 3     |       | none     | 95             | 80                     | 15                     |
| 4     |       | TBACl    | 93             | 20                     | 73                     |
| 5     |       | none     | 47             | 36                     | 11                     |
| 6     |       | TBACl    | 85             | 0                      | 85                     |
| 7     |       | none     | 63             | 58                     | 5                      |
| 8     |       | TBACl    | 49             | 0                      | 49                     |
| 9     |       | none     | 76             | 74                     | 2                      |
| 10    |       | TBACl    | 77             | 0                      | 77                     |

<sup>a</sup>Reaction conditions: In a thick-walled glass tube fitted with a Teflon cap, the catalyst was added to a 0.081 M solution of the secondary amine (0.081 mmol), phenylsilane (0.486 mmol), formic acid (0.243 mmol) in CH<sub>3</sub>CN (1 mL). The amount of TBACl used was 20 mol %. The reaction mixture was allowed to react at 80 °C for 3 h. Products were analyzed by <sup>1</sup>H NMR spectroscopy taking aliquots (20 μL) at the desired times using 1,3,5-trimethoxybenzene as integration standard. The results shown are the average between two runs.

is related to the amount of metal catalyst used. This result is important because some recent studies in the field of electrochemical reduction of CO<sub>2</sub> using [Mn(CNC)(CO)<sub>3</sub>]<sup>+</sup> complexes seem to suggest that the active catalytic species has a dimetallic nature.<sup>12</sup> In our case, the results support the monometallic nature of the active catalyst. On the basis of our observations and previous literature reports,<sup>32</sup> a tentative catalytic mechanism should involve a neutral hydride complex [(CNC)MnH(CO)<sub>2</sub>] (**A** in Scheme 2), formed by the reaction of the cationic [(CNC)Mn(CO)<sub>3</sub>]<sup>+</sup> complex in the presence of phenylsilane, with the concomitant formation of a silyl cation. Such types of Mn-hydrido complexes have been proposed as intermediates for the reduction of CO<sub>2</sub> and C=O bonds by Mn(I) tricarbonyl complexes supported by pincer ligands.<sup>28a,32,33</sup> However, this process is generally slow as it requires the irreversible loss of one CO ligand. We tried the ex-situ reaction of complex **2** with PhSiH<sub>3</sub> in dry acetonitrile, but the results were inconclusive, and the corresponding <sup>1</sup>H NMR spectra did not show signals at negative chemical shift values, as should be expected for Mn-hydrido complexes. The negligible activity of **2** in the reduction of formylated amine **5a** is likely due to its lack of ability to form the required Mn–H intermediate. In the case of the experiments performed with **2** with PhSiH<sub>3</sub> in the presence of TBACl, the formation of the paramagnetic complex resulting from the reduction of **2** prevented us from detecting the formation of the Mn–H complex by <sup>1</sup>H NMR spectroscopy. However, this Mn–H intermediate is very likely produced as it is generally considered a prerequisite for entering the reductive catalytic cycle.<sup>16a,28a,32,33</sup> As shown in Scheme 2 this manganese hydride

**Scheme 2. Tentative Reaction Mechanism for the Mn(I)-Catalyzed Hydrosilylation of Formamides**

(**A**) can catalyze hydride transfer from PhSiH<sub>3</sub> to the silyl-activated substrate (formed by the reaction of the silyl cation with the formylated amine) yielding the reaction intermediate **D** (Scheme 2). This intermediate can be further reduced via a second Mn-catalyzed hydride transfer to form the final methylated amine and a siloxane. While the exact nature of the catalytically active manganese-hydride **A** and how it enables the hydride transfer still needs to be elucidated, the proposed mechanism is in line with the currently available experimental data and previous mechanistic studies performed with similar cationic pincer Mn(I) carbonyl complexes and thus may serve as a working hypothesis for future studies.<sup>32a,34</sup>

While the cycle shown in Scheme 2 is redox-neutral on the manganese catalyst, combined experimental and computational calculations performed by Lan and Liu,<sup>34</sup> showed that manganese catalysts with more powerful electron-donating pincer ligands have a lower activation barrier for the hydrogen transfer from the metal hydride to the carbonyl group of the substrate (**B** in Scheme 2). In accordance with this, the greater electron-donating power of the NDI-functionalized pincer-CNC ligand in **2** was achieved upon the addition of the chloride anion (as a consequence of the one-electron reduction of the NDI moiety to form a NDI<sup>−</sup> radical monoanion), facilitates the hydrogen transfer step to the silyl-activated substrate (step **B**-to-**C** in Scheme 2). This justifies the better performance of catalyst **2** upon the addition of TBACl and suggests that this step is the rate-determining step (RDS) of the catalytic cycle.

We also performed another set of experiments aiming to compare the time-dependent reaction profiles of the catalytic reactions catalyzed by **2** alone, and by **2** in the presence of TBACl. As can be observed from the reaction profiles shown in Figure 3a, the reaction performed with **2** + TBACl was significantly more effective in the production of **5b** than that performed using **2** alone. In fact, the combination of **2** and TBACl produced **5b** quantitatively, while **2** alone was only capable of producing 8% of **5b** after 3 h of reaction. Interestingly, for the reaction catalyzed by the mixture of **2** + TBACl, no formylated product **5a** was detected all along the reaction process, indicating that the conversion of **5a** to **5b** by the catalyst in the presence of the silane is very fast. In a

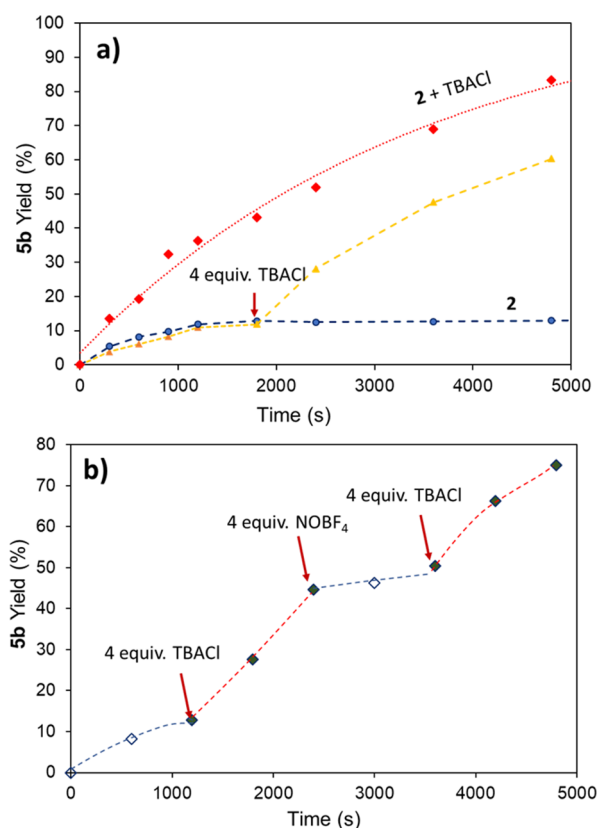


**Figure 3.** (a) Time-dependent reaction profiles of the methylation of *N*-ethylamine with formic acid in the presence of 6 equiv of  $\text{PhSiH}_3$  catalyzed by **2** (blue dots) and **2** + TBACl (red squares). The reactions were performed in  $\text{CH}_3\text{CN}$  at  $80^\circ\text{C}$ , using a 5 mol % of catalyst (**2**) loading. The amount of TBACl used was 20 mol %. The reaction profile depicted with the yellow triangles in (a) refers to a reaction that was initiated with **2** alone, and then TBACl was added after 30 min of reaction. The profile shown in (b) refers to a reaction initiated with **2** (5 mol %) and then subsequently activated and deactivated by addition of TBACl (4 equiv with respect to catalyst) and  $\text{NOBF}_4$  (4 equiv with respect to catalyst), respectively.

parallel experiment, we started the reaction using **2** alone and then added TBACl after 30 min of reaction. As can be seen from the resulting reaction profile shown in Figure 3a (yellow triangles), the activity of the catalyst was greatly enhanced after the addition of the halide additive. This experiment is a clear indication that the activity of the catalyst can be “switched on”, and that the “dormant” (or inactive) state of **2** can be “awoken” once the reaction has started by the addition of the chloride additive. It is also important to point out that once TBACl is added, the activity of the “activated” catalyst becomes exactly the same as the one shown when **2** + TBACl were used from the beginning, as the two lines defining the reaction profiles become parallel. In order to determine if we could toggle between the active and inactive forms of catalyst **2** several times along the reaction course, we performed a third experiment in which we followed the evolution of the reaction of methylation of *N*-ethylamine with formic acid using catalyst **2**, and then subsequently added four equivalents of TBACl and  $\text{NOBF}_4$  after periods of 20 min. As can be observed in the reaction profile shown in Figure 3b, the first addition of TBACl produces activation of the catalyst, which can be further deactivated by the addition of  $\text{NOBF}_4$ . The subsequent addition of four equivalents of TBACl reactivates the catalyst

until the completion of the reaction. This experiment shows that the catalyst can be “switched on” upon the addition of TBACl, and then “switched off” upon the addition of a mild oxidant such as  $\text{NOBF}_4$ . This observation provides clear evidence of the stability of the catalyst in both active/reduced and inactive/oxidized states and that the extended durations in the inactive form still allow the recovery of the activity upon oxidation. In addition, this experiment gives further support to our hypothesis that the rate-determining step of the catalytic cycle depicted in Scheme 2 is the hydrogen transfer step to the silyl-activated substrate (step B-to-C), as this step is known to be favored for pincer-Mn complexes with strong electron-donating ligands.<sup>3c</sup> In our case, the switching of the electron-donating power of the NDI-functionalized pincer ligand is effectively produced by the addition of chloride (catalyst ON, as a consequence of the one-electron reduction of the NDI moiety) and subsequent addition of  $\text{NOBF}_4$  (catalyst OFF, oxidation of the  $\text{NDI}^-$  anionic radical).

With these results in hand, we finally performed a series of catalytic reactions in which we used  $\text{CO}_2$  as a carbon source. The reactions were carried out with *N*-ethylaniline in the presence of 6 equiv of  $\text{PhSiH}_3$  using 5 mol % of **2** at  $110^\circ\text{C}$  under 10 atm of  $\text{CO}_2$  during 12 h. Under these reaction conditions, catalyst **2** alone produced 85% conversion of the substrate, with very little production of the methylated amine **5b** (8%). For the reaction performed with **2** + 4 equiv of TBACl, full conversion was obtained, with **5b** formed in 81% yield. Under these reaction conditions, the control experiment performed with 20 mol % of TBACl only produced 11 mol % of the targeted product **5b**.

## CONCLUSIONS

In summary, we prepared an Mn(I)-carbonyl complex with a pincer-CNC ligand functionalized with a naphthalene-diimide (NDI) moiety. The reduction of the NDI group results in an increase of the electron-donating strength of the pincer ligand, as was observed by the spectroelectrochemical experiments. We also observed that the addition of chloride anion produces the reduction of the NDI moiety attached to the pincer ligand, with the concomitant increase of the electron-donating power of the ligand, as reflected by the red-shift of the C–O stretching bands of the complex. This effect is translated into an important modification of the catalytic properties of the complex in the reductive *N*-methylation of several secondary amines with formic acid and  $\text{CO}_2$ . While the catalyst alone performs poorly, the combined action of the metal catalyst with tetrabutylammonium chloride results in a very effective catalyst that is able to selectively produce the methylated amine under relatively mild conditions. This catalytic enhancement is very likely due to the increase of the electron-donating power of the pincer ligand upon chloride addition, which facilitates the hydride transfer to the carbonyl group of the substrate, also reflecting that this step is the rate-determining step of the catalytic cycle. Furthermore, the activity of the catalyst can toggle between the activated and inactivated form for several cycles by adding subsequently TBACl and a mild oxidant such as  $\text{NOBF}_4$ .

Although we are aware that there are examples in the literature where more effective Mn-based catalysts for this process have been reported,<sup>10,28b</sup> our results highlight how the properties of a simple catalyst can be boosted by using anion-sensitive ligands as our NDI-functionalized pincer ligand, thus offering a new and simple way for tuning the catalytic activity

of homogeneous catalysts. We are confident that in the near future, anion-sensitive ligands will find a place in homogeneous catalysis similar to that already found for redox-, photo-, or pH-adaptive catalysts.

## ■ ASSOCIATED CONTENT

### SI Supporting Information

The Supporting Information is available free of charge at <https://pubs.acs.org/doi/10.1021/acscatal.4c01812>.

Experimental details concerning all catalytic studies and the electro-spectrochemical characterization of new complexes (PDF)

## ■ AUTHOR INFORMATION

### Corresponding Authors

**Macarena Poyatos** – Institute of Advanced Materials (INAM), Centro de Innovación en Química Avanzada (ORFEO–CINQA), Universitat Jaume I, E-12071 Castellón, Spain; [orcid.org/0000-0003-2000-5231](https://orcid.org/0000-0003-2000-5231); Email: [poyatosd@uji.es](mailto:poyatosd@uji.es)

**Eduardo Peris** – Institute of Advanced Materials (INAM), Centro de Innovación en Química Avanzada (ORFEO–CINQA), Universitat Jaume I, E-12071 Castellón, Spain; [orcid.org/0000-0001-9022-2392](https://orcid.org/0000-0001-9022-2392); Email: [eperis@uji.es](mailto:eperis@uji.es)

### Authors

**Sebastián Martínez-Vivas** – Institute of Advanced Materials (INAM), Centro de Innovación en Química Avanzada (ORFEO–CINQA), Universitat Jaume I, E-12071 Castellón, Spain

**Sergio Gonell** – Institute of Advanced Materials (INAM), Centro de Innovación en Química Avanzada (ORFEO–CINQA), Universitat Jaume I, E-12071 Castellón, Spain; [orcid.org/0000-0003-0517-6833](https://orcid.org/0000-0003-0517-6833)

Complete contact information is available at: <https://pubs.acs.org/10.1021/acscatal.4c01812>

### Author Contributions

The manuscript was written through contributions of all authors. All authors have given approval to the final version of the manuscript.

### Funding

Ministerio de Ciencia y Universidades (PID2021–127862NB-I00 and TED2021–130647B–I00), and Universitat Jaume I (UJI-B2020–01 and UJI-B2021–39).

### Notes

The authors declare no competing financial interest.

## ■ ACKNOWLEDGMENTS

We gratefully acknowledge financial support from the Ministerio de Ciencia y Universidades (PID2021–127862NB-I00 and TED2021–130647B–I00) and the Universitat Jaume I (UJI-B2020–01 and UJI-B2021–39). We are grateful to the Serveis Centrals d'Instrumentació Científica (SCIC-UJI) for providing spectroscopic facilities.

## ■ ABBREVIATIONS

NDI, naphthalene-diimide; NHC, N-heterocyclic carbene; TBACl, tetrabutylammonium chloride

## ■ REFERENCES

- (1) (a) Carney, J. R.; Dillon, B. R.; Thomas, S. P. Recent Advances of Manganese Catalysis for Organic Synthesis. *Eur. J. Org. Chem.* **2016**, *2016*, 3912–3929. (b) Valyaev, D. A.; Lavigne, G.; Lugan, N. Manganese organometallic compounds in homogeneous catalysis: Past, present, and prospects. *Coord. Chem. Rev.* **2016**, *308*, 191–235. (c) Garbe, M.; Junge, K.; Beller, M. Homogeneous Catalysis by Manganese-Based Pincer Complexes. *Eur. J. Org. Chem.* **2017**, *2017*, 4344–4362. (d) Grills, D. C.; Ertem, M. Z.; McKinnon, M.; Ngo, K. T.; Rochford, J. Mechanistic aspects of CO<sub>2</sub> reduction catalysis with manganese-based molecular catalysts. *Coord. Chem. Rev.* **2018**, *374*, 173–217. (e) Hu, Y.; Zhou, B.; Wang, C. Inert C–H Bond Transformations Enabled by Organometallic Manganese Catalysis. *Acc. Chem. Res.* **2018**, *51*, 816–827. (f) Kallmeier, F.; Kempe, R. Manganese Complexes for (De)Hydrogenation Catalysis: A Comparison to Cobalt and Iron Catalysts. *Angew. Chem., Int. Ed.* **2018**, *57*, 46–60. (g) Mukherjee, A.; Milstein, D. Homogeneous Catalysis by Cobalt and Manganese Pincer Complexes. *ACS Catal.* **2018**, *8*, 11435–11469.
- (2) Petersen, H. A.; Myren, T. H. T.; O'Sullivan, S. J.; Luca, O. R. Electrochemical methods for materials recycling. *Mater. Adv.* **2021**, *2*, 1113–1138.
- (3) (a) Peris, E.; Crabtree, R. H. Key factors in pincer ligand design. *Chem. Soc. Rev.* **2018**, *47*, 1959–1968. (b) Bertini, F.; Glatz, M.; Stoeger, B.; Peruzzini, M.; Veiros, L. F.; Kirchner, K.; Gonsalvi, L. Carbon Dioxide Reduction to Methanol Catalyzed by Mn(I) PNP Pincer Complexes under Mild Reaction Conditions. *ACS Catal.* **2019**, *9*, 632–639. (c) Schlichter, P.; Werle, C. The Rise of Manganese-Catalyzed Reduction Reactions. *Synthesis-Stuttgart* **2022**, *54*, 517–534.
- (4) Gomes, C. D.; Jacquet, O.; Villiers, C.; Thuéry, P.; Ephritikhine, M.; Cantat, T. A Diagonal Approach to Chemical Recycling of Carbon Dioxide: Organocatalytic Transformation for the Reductive Functionalization of CO<sub>2</sub>. *Angew. Chem., Int. Ed.* **2012**, *51*, 187–190.
- (5) Agarwal, J.; Shaw, T. W.; Stanton, C. J.; Majetich, G. F.; Bocarsly, A. B.; Schaefer, H. F. NHC-Containing Manganese(I) Electrocatalysts for the Two-Electron Reduction of CO<sub>2</sub>. *Angew. Chem., Int. Ed.* **2014**, *53*, 5152–5155.
- (6) Agarwal, J.; Stanton, C. J.; Shaw, T. W.; Vandezande, J. E.; Majetich, G. F.; Bocarsly, A. B.; Schaefer, H. F. Exploring the effect of axial ligand substitution (X = Br, NCS, CN) on the photo-decomposition and electrochemical activity of MnX(N–C)(CO)<sub>3</sub> complexes. *Dalton Trans.* **2015**, *44*, 2122–2131.
- (7) Stanton, C. J.; Vandezande, J. E.; Majetich, G. F.; Schaefer, H. F.; Agarwal, J. Mn–NHC Electrocatalysts: Increasing  $\pi$  Acidity Lowers the Reduction Potential and Increases the Turnover Frequency for CO<sub>2</sub> Reduction. *Inorg. Chem.* **2016**, *55*, 9509–9512.
- (8) Franco, F.; Pinto, M. F.; Royo, B.; Lloret-Fillol, J. A Highly Active N-Heterocyclic Carbene Manganese(I) Complex for Selective Electrocatalytic CO<sub>2</sub> Reduction to CO. *Angew. Chem., Int. Ed.* **2018**, *57*, 4603–4606.
- (9) Fernández, S.; Franco, F.; Belmonte, M. M.; Friaes, S.; Royo, B.; Luis, J. M.; Lloret-Fillol, J. Decoding the CO<sub>2</sub> Reduction Mechanism of a Highly Active Organometallic Manganese Electrocatalyst: Direct Observation of a Hydride Intermediate and Its Implications. *ACS Catal.* **2023**, *13*, 10375–10385.
- (10) Masaro, C.; Meloni, G.; Baron, M.; Graiff, C.; Tubaro, C.; Royo, B. Bis-N-Heterocyclic Carbene Manganese(I) Complexes in Catalytic N-Formylation N-Methylation of Amines Using Carbon Dioxide and Phenylsilane. *Chem.—Eur. J.* **2023**, *29*, No. e202302273.
- (11) (a) Myren, T. H. T.; Lilio, A. M.; Huntzinger, C. G.; Horstman, J. W.; Stinson, T. A.; Donadt, T. B.; Moore, C.; Lama, B.; Funke, H. H.; Luca, O. R. Manganese N-Heterocyclic Carbene Pincers for the Electrocatalytic Reduction of Carbon Dioxide. *Organometallics* **2019**, *38*, 1248–1253. (b) Myren, T. H. T.; Atherz, A.; Stinson, T. A.; Huntzinger, C. G.; Lama, B.; Musgrave, C. B.; Luca, O. R. Metalloradical intermediates in electrocatalytic reduction of CO<sub>2</sub> to CO: Mn versus Re bis-N-heterocyclic carbene pincers. *Dalton Trans.* **2020**, *49*, 2053–2057.

- (12) Myren, T. H. T.; Alherz, A.; Thurston, J. R.; Stinson, T. A.; Huntzinger, C. G.; Musgrave, C. B.; Luca, O. R. Mn-Based Molecular Catalysts for the Electrocatalytic Disproportionation of CO<sub>2</sub> into CO and CO<sub>3</sub><sup>2-</sup>. *ACS Catal.* **2020**, *10*, 1961–1968.
- (13) Huang, C.; Liu, J. H.; Huang, H. H.; Xu, X. F.; Ke, Z. F. Highly active electrocatalytic CO<sub>2</sub> reduction with manganese N-heterocyclic carbene pincer by *para* electronic tuning. *Chin. Chem. Lett.* **2022**, *33*, 262–265.
- (14) (a) Hock, S. J.; Schaper, L. A.; Herrmann, W. A.; Kühn, F. E. Group 7 transition metal complexes with N-heterocyclic carbenes. *Chem. Soc. Rev.* **2013**, *42*, 5073–5089. (b) Bellemin-Laponnaz, S.; Dagonne, S. Group 1 and 2 and Early Transition Metal Complexes Bearing N-Heterocyclic Carbene Ligands: Coordination Chemistry, Reactivity, and Applications. *Chem. Rev.* **2014**, *114*, 8747–8774. (c) Friaes, S.; Realista, S.; Mourao, H.; Royo, B. N-Heterocyclic and Mesoionic Carbenes of Manganese and Rhenium in Catalysis. *Eur. J. Inorg. Chem.* **2022**, *2022*, No. e202100884.
- (15) (a) Valyaev, D. A.; Wei, D.; Elangovan, S.; Cavailles, M.; Dorcet, V.; Sortais, J. B.; Darcel, C.; Lugan, N. Half-Sandwich Manganese Complexes Bearing Cp Tethered N-Heterocyclic Carbene Ligands: Synthesis and Mechanistic Insights into the Catalytic Ketone Hydrosilylation. *Organometallics* **2016**, *35*, 4090–4098. (b) Zheng, J. X.; Elangovan, S.; Valyaev, D. A.; Brousses, R.; César, V.; Sortais, J. B.; Darcel, C.; Lugan, N.; Lavigne, G. Hydrosilylation of Aldehydes and Ketones Catalyzed by Half-Sandwich Manganese(I) N-Heterocyclic Carbene Complexes. *Adv. Synth. Catal.* **2014**, *356*, 1093–1097. (c) Sousa, S. C. A.; Carrasco, C. J.; Pinto, M. F.; Royo, B. A Manganese N-Heterocyclic Carbene Catalyst for Reduction of Sulfoxides with Silanes. *ChemCatChem* **2019**, *11*, 3839–3843. (d) Sousa, S. C. A.; Realista, S.; Royo, B. Bench-Stable Manganese NHC Complexes for the Selective Reduction of Esters to Alcohols with Silanes. *Adv. Synth. Catal.* **2020**, *362*, 2437–2443. (e) Pinto, M.; Friaes, S.; Franco, F.; Lloret-Fillol, J.; Royo, B. Manganese N-Heterocyclic Carbene Complexes for Catalytic Reduction of Ketones with Silanes. *ChemCatChem* **2018**, *10*, 2734–2740.
- (16) (a) Yang, W. J.; Chernyshov, I. Y.; van Schendel, R. K. A.; Weber, M.; Mueller, C.; Filonenko, G. A.; Pidko, E. A. Robust and efficient hydrogenation of carbonyl compounds catalysed by mixed donor Mn(I) pincer complexes. *Nat. Commun.* **2021**, *12*, 12. (b) Wei, Z. Y.; Li, H. X.; Wang, Y. J.; Liu, Q. A Tailored Versatile and Efficient NHC-Based NNC-Pincer Manganese Catalyst for Hydrogenation of Polar Unsaturated Compounds. *Angew. Chem., Int. Ed.* **2023**, *62*, No. e2023010. (c) Both, N. F.; Spannenberg, A.; Jiao, H. J.; Junge, K.; Beller, M. Bis(N-Heterocyclic Carbene) Manganese(I) Complexes: Efficient and Simple Hydrogenation Catalysts. *Angew. Chem., Int. Ed.* **2023**, *62*, No. e202307987.
- (17) (a) Bhosale, S. V.; Jani, C. H.; Langford, S. J. Chemistry of naphthalene diimides. *Chem. Soc. Rev.* **2008**, *37*, 331–342. (b) Bhosale, S. V.; Al Kobaisi, M.; Jadhav, R. W.; Morajkar, P. P.; Jones, L. A.; George, S. Naphthalene diimides: perspectives and promise. *Chem. Soc. Rev.* **2021**, *50*, 9845–9998.
- (18) (a) Schottel, B. L.; Chifotides, H. T.; Dunbar, K. R. Anion- $\pi$  interactions. *Chem. Soc. Rev.* **2008**, *37*, 68–83. (b) Dawson, R. E.; Hennig, A.; Weimann, D. P.; Emery, D.; Ravikumar, V.; Montenegro, J.; Takeuchi, T.; Gabutti, S.; Mayor, M.; Mareda, J.; Schalley, C. A.; Matile, S. Experimental evidence for the functional relevance of anion- $\pi$  interactions. *Nat. Chem.* **2010**, *2*, 533–538. (c) Ballester, P. Experimental Quantification of Anion- $\pi$  Interactions in Solution Using Neutral Host-Guest Model Systems. *Acc. Chem. Res.* **2013**, *46*, 874–884. (d) Watt, M. M.; Collins, M. S.; Johnson, D. W. Ion- $\pi$  Interactions in Ligand Design for Anions and Main Group Cations. *Acc. Chem. Res.* **2013**, *46*, 955–966.
- (19) (a) Ajayakumar, M. R.; Mukhopadhyay, P.; Yadav, S.; Ghosh, S. Single-Electron Transfer Driven Cyanide Sensing: A New Multimodal Approach. *Org. Lett.* **2010**, *12*, 2646–2649. (b) Ajayakumar, M. R.; Asthana, D.; Mukhopadhyay, P. Core-Modified Naphthalenediimides Generate Persistent Radical Anion and Cation: New Panchromatic NIR Probes. *Org. Lett.* **2012**, *14*, 4822–4825. (c) Zhao, J. F.; Li, G.; Wang, C. Y.; Chen, W. Q.; Chye, S.; Loo, J.; Zhang, Q. C. A new N-substituted heteroacene can detect CN<sup>-</sup> and F<sup>-</sup> anions via anion- $\pi$  interaction. *RSC Adv.* **2013**, *3*, 9653–9657. (d) Mitra, A.; Clark, R. J.; Hubley, C. T.; Saha, S. Anion- $\pi$  and CH $\cdots$  anion interactions in naphthalenediimide-based coordination complexes. *Supramol. Chem.* **2014**, *26*, 296–301. (e) Giese, M.; Albrecht, M.; Rissanen, K. Experimental investigation of anion- $\pi$  interactions - applications and biochemical relevance. *Chem. Commun.* **2016**, *52*, 1778–1795. (f) Zhao, Y. J.; Cotellet, Y.; Sakai, N.; Matile, S. Unorthodox Interactions at Work. *J. Am. Chem. Soc.* **2016**, *138*, 4270–4277.
- (20) (a) Ruiz-Zambrana, C.; Gutierrez-Blanco, A.; Gonell, S.; Poyatos, M.; Peris, E. Redox-Switchable Cycloisomerization of Alkynoic Acids with Naphthalenediimide-Derived N-Heterocyclic Carbene Complexes. *Angew. Chem., Int. Ed.* **2021**, *60*, 20003–20011. (b) Gutierrez-Pena, C. L.; Poyatos, M.; Peris, E. A redox-switchable catalyst with an ‘unplugged’ redox tag. *Chem. Commun.* **2022**, *58*, 10564–10567.
- (21) Ruiz-Zambrana, C.; Poyatos, M.; Peris, E. A redox-switchable gold(I) complex for the hydroamination of acetylenes: a convenient way for studying ligand-derived electronic effects. *ACS Catal.* **2022**, *12*, 4465–4472.
- (22) Martínez-Vivas, S.; Gusev, D. G.; Poyatos, M.; Peris, E. Tuning the Catalytic Activity of a Pincer Complex of Rhodium(I) by Supramolecular and Redox Stimuli. *Angew. Chem., Int. Ed.* **2023**, *62*, No. e202313899.
- (23) Stanton, C. J., III; Machan, C. W.; Vandezande, J. E.; Jin, T.; Majetich, G. F.; Schaefer, H. F., III; Kubiak, C. P.; Li, G.; Agarwal, J. Re(I) NHC Complexes for Electrocatalytic Conversion of CO<sub>2</sub>. *Inorg. Chem.* **2016**, *55*, 3136–3144.
- (24) Guha, S.; Goodson, F. S.; Corson, L. J.; Saha, S. Boundaries of Anion/Naphthalenediimide Interactions: From Anion- $\pi$  Interactions to Anion-Induced Charge-Transfer and Electron-Transfer Phenomena. *J. Am. Chem. Soc.* **2012**, *134*, 13679–13691.
- (25) Sorribes, I.; Junge, K.; Beller, M. General Catalytic Methylation of Amines with Formic Acid under Mild Reaction Conditions. *Chem.—Eur. J.* **2014**, *20*, 7878–7883.
- (26) (a) Naik, G.; Sarki, N.; Goyal, V.; Narani, A.; Natte, K. Recent Trends in Upgrading of CO<sub>2</sub> as a C1 Reactant in N- and C-Methylation Reactions. *Asian J. Org. Chem.* **2022**, *11*, No. e2022002. (b) Goyal, V.; Naik, G.; Narani, A.; Natte, K.; Jagadeesh, R. V. Recent developments in reductive N-methylation with base-metal catalysts. *Tetrahedron* **2021**, *98*, No. 132414. (c) Zhang, Y.; Zhang, T.; Das, S. Catalytic transformation of CO<sub>2</sub> into C1 chemicals using hydrosilanes as a reducing agent. *Green Chem.* **2020**, *22*, 1800–1820.
- (27) Jacquet, O.; Gomes, C. D. N.; Ephritikhine, M.; Cantat, T. Recycling of Carbon and Silicon Wastes: Room Temperature Formylation of N-H Bonds Using Carbon Dioxide and Polymethylhydrosiloxane. *J. Am. Chem. Soc.* **2012**, *134*, 2934–2937.
- (28) (a) Kostera, S.; Manca, G.; Gonsalvi, L. Carbon Dioxide Hydrogenation to Formate Catalyzed by a Neutral, Coordinatively Saturated Tris-Carbonyl Mn(I)-PNP Pincer-Type Complex. *Chem.—Eur. J.* **2023**, *29*, No. e202302642. (b) Huang, Z. J.; Jiang, X. L.; Zhou, S. F.; Yang, P. J.; Du, C. X.; Li, Y. H. Mn-Catalyzed Selective Double and Mono-N-Formylation and N-Methylation of Amines by using CO<sub>2</sub>. *ChemSusChem* **2019**, *12*, 3054–3059. (c) Papa, V.; Cabrero-Antonino, J. R.; Alberico, E.; Spanneberg, A.; Junge, K.; Junge, H.; Beller, M. Efficient and selective hydrogenation of amides to alcohols and amines using a well-defined manganese-PNN pincer complex. *Chem. Sci.* **2017**, *8*, 3576–3585. (d) Kar, S.; Goepfert, A.; Kothandaraman, J.; Prakash, G. K. S. Manganese-Catalyzed Sequential Hydrogenation of CO<sub>2</sub> to Methanol via Formamide. *ACS Catal.* **2017**, *7*, 6347–6351. (e) Kelly, C. M.; McDonald, R.; Sydora, O. L.; Stradiotto, M.; Turculet, L. A Manganese Pre-Catalyst: Mild Reduction of Amides, Ketones, Aldehydes, and Esters. *Angew. Chem., Int. Ed.* **2017**, *56*, 15901–15904.
- (29) Frogneux, X.; Jacquet, O.; Cantat, T. Iron-catalyzed hydro-silylation of CO<sub>2</sub>: CO<sub>2</sub> conversion to formamides and methylamines. *Catal. Sci. Technol.* **2014**, *4*, 1529–1533.



(30) Liu, X. F.; Ma, R.; Qiao, C.; Cao, H.; He, L. N. Fluoride-Catalyzed Methylation of Amines by Reductive Functionalization of CO<sub>2</sub> with Hydrosilanes. *Chem.—Eur. J.* **2016**, *22*, 16489–16493.

(31) (a) Bures, J. A Simple Graphical Method to Determine the Order in Catalyst. *Angew. Chem., Int. Ed.* **2016**, *55*, 2028–2031.

(b) Bures, J. Variable Time Normalization Analysis: General Graphical Elucidation of Reaction Orders from Concentration Profiles. *Angew. Chem., Int. Ed.* **2016**, *55*, 16084–16087.

(32) (a) Martinez-Ferrate, O.; Chatterjee, B.; Werle, C.; Leitner, W. Hydrosilylation of carbonyl and carboxyl groups catalysed by Mn(I) complexes bearing triazole ligands. *Catal. Sci. Technol.* **2019**, *9*, 6370–6378. (b) Huang, J.; Sun, F.; Liu, W. Manganese-catalyzed deoxygenation of secondary and tertiary amides under mild conditions. *J. Catal.* **2023**, *423*, 19–25.

(33) Wei, Z.; Li, H.; Wang, Y.; Liu, Q. A Tailored Versatile and Efficient NHC-Based NNC-Pincer Manganese Catalyst for Hydrogenation of Polar Unsaturated Compounds. *Angew. Chem., Int. Ed.* **2023**, *62*, No. e202301042.

(34) Wang, Y.; Zhu, L.; Shao, Z.; Li, G.; Lan, Y.; Liu, Q. Unmasking the Ligand Effect in Manganese-Catalyzed Hydrogenation: Mechanistic Insight and Catalytic Application. *J. Am. Chem. Soc.* **2019**, *141*, 17337–17349.